# Azobenzimidazole Compounds and Polymers for Nonlinear Optics

**Elisa M. Cross,* Kenneth M. White, Robert S. Moshrefzadeh, and Cecil V. Francis**

*3M Corporate Research Laboratory, Building 201-2E-08, St. Paul, Minnesota 55144-1000*

*Received July 21, 1994; Revised Manuscript Received November 21, 1994®*

ABSTRACT: Novel difunctional nonlinear optical (NLO) azo compounds with exceptional thermal stability have been synthesized and incorporated into side-chain and cross-linked polymers. The nonlinear optical response of these polymers has been studied with second-harmonic generation and electrooptic measurements. Channel waveguide intensity modulators displayed an electrooptic coefficient of 13.1 pm/V.

## Introduction

Organic polymers with stable second-order optical nonlinearity are desired for use in electrooptical devices. An increasing number of publications have appeared in which the orientational stability is being improved by the use of cross-linked polymers. These nonlinear optical (NLO)-active cross-linked polymers can be divided into two classes: those in which the NLO chromophore is attached to the polymer network at one end (cross-linking is around the NLO chromophore) and those in which the NLO chromophore is attached at more than one point (the NLO chromophore is a cross-link). Several reports of the first class of material have appeared, and modest improvements in the maintenance of dipole orientation at elevated temperatures were observed.[1−12]

More recently, many reports of the second class of cross-linked NLO-active materials have appeared.[13−24] These reports discuss materials which incorporate NLO chromophores of high nonlinearity and good stability at elevated temperatures into cross-linked matrices by attachment at both the electron-donor and the electron-acceptor ends. The increase in orientational stability resulting from cross-linking has been established by several reports which compare second-harmonic generation (SHG) stability of polymers before and after cross-linking.[20−22] Stability of NLO response at temperatures as high as 125 °C has been observed.[21,22] This degree of stability was achieved by Xu *et al.* using "double-ended chromophores"—molecules with two different polymerizable functionalities at each end of the NLO chromophore. A similar scheme involving stepwise polymerization of two functionalities to give NLO-active cross-linked polymers was recently reported by Beecher *et al.*[24]

We have reported optically nonlinear materials made by incorporating 3-amino-5-[4-(*N*-ethyl-*N*-(2-hydroxyethyl)amino]benzylidene]rhodanine (RA) into a cross-linked polymer via stepwise reaction of amino and hydroxyl groups with a trifunctional isocyanate.[25−27] This molecule, with a hydroxyl group at the electron-donor end and an amino group at the electron-acceptor end, is similar in principle to the double-ended chromophores described above. However, while those materials comprise molecules which can be cross-linked by stepwise polymerization of two functionalities, different polymerization mechanisms must be used. In contrast, the functional groups on RA were reacted stepwise with the same reagent, a trifunctional isocyanate (Tolonate HDT). The hydroxyl and amino functional groups of RA are cross-linked by the same mechanism, although at vastly differing rates due to their differing reactivity.

With the cross-linked RA−HDT system, very little relaxation of the noncentrosymmetric alignment was observed, even at 100 °C for extended periods of time. The decrease in SHG that was observed revealed another practical problem with most systems studied for their optically nonlinear properties—thermal instability of common NLO chromophores. We believe that nearly all of the SHG decay observed in the RA−HDT material was due to thermal instability of the NLO chromophore.[25,27] Other molecules we developed for NLO materials, such as nitrophenylbarbituric acid derivatives,[26,28] had very high $\mu\beta$ values but were also found to degrade upon extended heating in polymer films. Instability of NLO chromophores, which has been observed by other researchers as well,[29−31] is critical for device operation for very long times at temperatures ranging from −40 to +80 °C.

The molecules reported herein resulted from our search for molecules with good thermal stability as well as high NLO activity, good solubility, difunctionality, and easy synthesis. The compounds are azo dyes, employing a functionalized nitrobenzimidazole group as the electron acceptor. A preliminary account of this work has been published.[32] The benzimidazole structure was chosen because poly(benzimidazoles) are known to be very stable high-temperature polymers[33] and because the trivalent imidazole nitrogen offers a site for functionalization of the molecule. The chemistry and synthesis of both benzimidazoles[34] and azo compounds[35] are well-known, as are diazotizations of amino-functional benzimidazoles.[34] The azobenzimidazoles described here exhibited excellent thermal stability as well as high optical nonlinearity and are easily synthesized with different functionalities at each end of the molecule.

These azobenzimidazoles have been incorporated into cross-linked NLO-active polymers by reaction of an aminohydroxy functional compound with Tolonate HDT, as was done for RA. In addition, functionalized linear polymers have been made which can be cross-linked analogously to the double-ended chromophore materials. The synthesis, thermal stability, and NLO properties of these azobenzimidazole compounds and polymers will be discussed here. In addition, results from the fabrication of Mach−Zehnder devices will be presented.

® Abstract published in *Advance ACS Abstracts,* February 15, 1995.

0024-9297/95/2228-2526$09.00/0 

**Scheme 1. Synthesis of Azobenzimidazole Compounds**

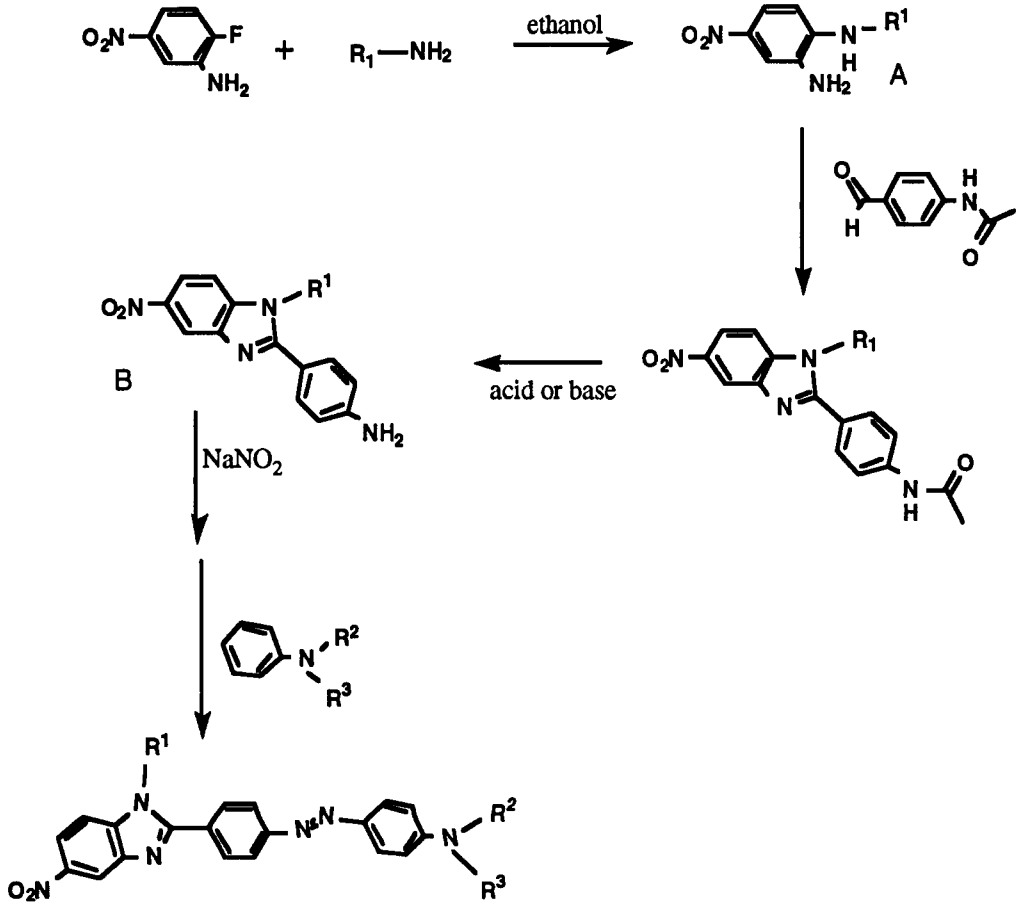


| | $R^1$ | $R^2$ | $R^3$ |
|---|---|---|---|
| **BI** | $CH_2CH(CH_3)OH$ | $CH_2CH_2OH$ | $CH_2CH_3$ |
| **BIN2** | $CH_2CH_2NH_2$ | $CH_2CH_2OH$ | $CH_2CH_3$ |
| **3** | $CH_2CH_2OH$ | $CH_2CH_3$ | $CH_2CH_3$ |
| **4** | $CH_2CH(CH_3)OH$ | $CH_2CH_3$ | $CH_2CH_3$ |
| **5** | $CH_2CH(CH_3)OH$ | $CH_2CH_2NH_2$ | $CH_2CH_3$ |
| **6** | $CH_2CH_2OH$ | $CH_2CH_2NH_2$ | $CH_2CH_3$ |
| **7** | $CH_2CH_2OH$ | $CH_2CH(CH_3)OH$ | $CH_2CH(CH_3)OH$ |
| **8** | $CH_2CH_2NH_2$ | $CH_2CH_2OH$ | $CH_2CH_2OH$ |
| **9** | $CH_2CH(CH_3)OH$ | $CH_2CH(CH_3)OH$ | $CH_2CH(CH_3)OH$ |
| **10** | $CH_2CH_2OH$ | $CH_2CH_2NHC(O)CH_2CH_3$ | $CH_2CH_3$ |
| **11** | $CH_2CH_2OH$ | $CH_2CH_2OC(O)NHCH_2CH_2OC(O)C(CH_3)=CH_2$ | $CH_2CH_3$ |
| **12** | $CH_2CH(CH_3)OH$ | $CH_2CH_2OC(O)C(CH_3)=CH_2$ | $CH_2CH_3$ |
| **13** | $CH_2CH(CH_3)OH$ | $CH_2CH_2OC(O)NHCH_2CH_2OC(O)C(CH_3)=CH_2$ | $CH_2CH_3$ |
| **14** | $CH_2CH_2NH_2$ | $CH_2CH_2NH_2$ | $CH_2CH_3$ |

## Experimental Section

**Synthesis.** Azobenzimidazole compounds were synthesized according to Scheme 1. Substituted 2-amino-5-nitroanilines (**A**), prepared by reactions of 2-fluoro-5-nitroaniline with primary amines, were reacted with *p*-acetamidobenzaldehyde and hydrolyzed to yield 1-substituted 2-(4-aminophenyl)-5-nitrobenzimidazoles (**B**). Direct formation of benzimidazoles from aldehydes and phenylenediamines as performed here was described by Stephens and Bower.[38] Diazotization of compounds (**B**) and coupling with the appropriate aniline gave the azobenzimidazoles (BI, BIN2, and **3**–**14**). Representative experimental procedures for each step of the synthesis are given below, using BIN2 as an example. $^1$H NMR and melting point data for compounds which are not included here were submitted as supplementary material.

2-(*N*-Ethylanilino)ethanol, *N*,*N*-diethylaniline, and *N*-phenyldiethanolamine were used as received from Aldrich Chemical Co. *N*,*N*-Bis(2-hydroxypropyl)aniline was used as received from Aldrich Chemical. *N*-(2-Aminoethyl)-*N*-ethylaniline (used in the synthesis of **5** and **6**) and *N*-(2-acetamidoethyl)-*N*-ethylaniline (used in the synthesis of **10**) were synthesized by the method of Fazio.[37] 2-(*N*-Ethylanilino)ethyl *N*-[2-(methacryloyloxy)ethyl]carbamate (used in the synthesis of **11** and **13**) and *N*-ethyl-*N*-[2-(methacryloyloxy)ethyl]aniline (used in the synthesis of **12**) were synthesized as below.

**2-(2-Aminoethyl)amino-5-nitroaniline (A, $R^1$ = $CH_2CH_2NH_2$).** A solution of 100 g (0.641 mol) of 2-fluoro-5-nitro-

aniline in 150 g (2.5 mol) of ethylenediamine and 350 mL of ethanol was refluxed for approximately 16 h. The hot solution was filtered to remove the ethanol-insoluble side product *N,N'*-bis(2-aminophenyl)ethylenediamine. The filtrate was cooled, and the 2-(2-aminoethyl)amino-5-nitroaniline (mp 132–135 °C) was collected and rinsed with ethanol. The yield was 89 g (68%). $^1$H NMR (DMSO-$d_6$): $\delta$ 7.51 (d, 1H, ArH), 7.40 (s, 1H, ArH), 6.50 (d, 1H, ArH), 5.89 (s, 1H, NH), 5.15 (s, 2H, $NH_2$), 3.20 (q, 2H, $CH_2$), 2.75 (t, 2H, $CH_2$), 1.5–2.5 (br, 2H, $NH_2$).

**1-(2-Aminoethyl)-2-(4-aminophenyl)-5-nitrobenzimidazole (B, R$^1$ = $CH_2CH_2NH_2$).** A solution of 20.6 g (0.10 mol) of 2-(2-aminoethyl)amino-5-nitroaniline and 16.6 g (0.10 mol) of *p*-acetamidobenzaldehyde in 100 mL of acetic acid was refluxed for approximately 16 h. The solution was cooled, and water was added until a precipitate formed. A pale yellow solid (21.5 g, 57% yield), spectroscopically confirmed as 1-(2-acetamidoethyl)-2-(4-acetamidophenyl)-5-nitrobenzimidazole, was collected and rinsed with water. $^1$H NMR (DMSO-$d_6$): $\delta$ 10.26 (s, 1H, NH), 8.52 (s, 1H, ArH), 8.20 (d, 1H, ArH), 7.90 (t, 1H, NH), 7.85–7.70 (m, 6H, ArH), 4.40 (t, 2H, $CH_2$), 3.35 (t, 2H, $CH_2$), 2.10 (s, 3H, $CH_3$), 1.55 (s, 3H, $CH_3$).

A 7.5 g (20 mmol) portion of the above product was added to a mixture of 40 mL of water, 10 mL of concentrated HCl, and 20 mL of ethanol, and the solution was refluxed for approximately 16 h. After the solution cooled, an aqueous 1.0 M NaOH solution was used to neutralize the pH. A dark yellow solid (mp 204–206 °C) was obtained in 72% yield. $^1$H NMR (DMSO-$d_6$): $\delta$ 8.48 (s, 1H, ArH), 8.28 (d, 1H, ArH), 7.80 (d, 1H, ArH), 7.55 (d, 2H, ArH), 6.70 (d, 2H, ArH), 5.75 (s, 2H, $NH_2$), 4.44 (t, 2H, $CH_2$), 3.0 (t, 2H, $CH_2$).

**1-(2-Aminoethyl)-2-[4-[4-[*N*-(2-hydroxyethyl)-*N*-ethylamino]phenyl]azo]phenyl]-5-nitrobenzimidazole (BIN2).** In 200 mL of concentrated HCl was dissolved 30.47 g (0.10 mol) of 1-(2-aminoethyl)-2-(4-aminophenyl)-5-nitrobenzimidazole. To this solution was added 200 mL of ice water, and the solution was cooled in an ice bath. Sodium nitrite (7.3 g, 0.10 mol) in 50 mL of water was added slowly while the temperature was kept below 10 °C. To the resulting solution was added a third solution of 16.98 g (0.10 mol) of 2-(*N*-ethylanilino)ethanol in 50 mL of ethanol. The purple solution was then poured into 200 mL of ice water and neutralized with 2 N NaOH, while ice was added as required to keep the temperature below 10 °C. As the pH was neutralized, an orange precipitate formed. The solid was collected and added to 600 mL of ethanol. This slurry was heated to reflux. The ethanol-insoluble product (38 g) was collected and rinsed with hot ethanol. At this point the material exhibited two spots by thin-layer chromatography. Recrystallization from pyridine yielded 13.0 g of the pure compound (mp 198 °C, 24% yield). $^1$H NMR (DMSO-$d_6$): $\delta$ 8.60 (s, 1H, ArH), 8.23 (d, 1H, ArH), 8.08 (d, 2H, ArH), 7.95 (m, 3H, ArH), 7.80 (d, 2H, ArH), 6.85 (d, 2H, ArH), 4.86 (br, 1H, OH), 4.40 (t, 2H, $CH_2$), 3.62 (t, 2H, $CH_2$), 3.51 (m, 4H, $CH_2$), 2.92 (t, 2H, $CH_2$), 1.18 (t, 3H, $CH_3$).

**2-(*N*-Ethylanilino)ethyl *N*-[2-(Methacryloyloxy)ethyl]-carbamate.** 2-(*N*-Ethylanilino)ethanol (31.1 g, 0.188 mol) and 2-isocyanatoethyl methacrylate (29 mL, used as obtained from Dow Chemical) were added to 125 mL of dry pyridine. Catalytic amounts of triethylenediamine and dibutyltin dilaurate were added. The solution became warm. After 10 min the reaction was shown to be complete by thin-layer chromatography, and the pyridine was removed with a rotoevaporator, yielding a colorless oil. The yield was 55 g or 92%. $^1$H NMR DMSO-$d_6$): $\delta$ 7.4 (t, 1H, NH), 7.15 (t, 2H, ArH), 6.7 (d, 2H, ArH), 6.55 (t, 1H, ArH), 6.05 (s, 1H, vinyl), 5.68 (s, 1H, vinyl), 4.05 (q, 4H, $CH_2$), 3.45 (t, 2H, $CH_2$), 3.35 (q, 2H, $CH_2$), 3.30 (q, 2H, $CH_2$).

***N*-Ethyl-*N*-[2-(methacryloyloxy)ethyl]aniline.** 2-(*N*-Ethylanilino)ethanol (26.60 g, 0.15 mol) was dissolved in 75 mL of dry pyridine. Methacrylic anhydride (28 mL, 0.18 mol) and a catalytic amount of 4-(dimethylamino)pyridine (Aldrich) were added. The solution was refluxed for 0.5 h, at which time thin-layer chromatography showed the reaction to be complete. The pyridine was removed via rotoevaporator. The residue was dissolved in ethyl acetate and extracted three times with a 0.1 N $NaHCO_3$ solution, dried over $MgSO_4$, and reduced. The liquid product (30.1 g, 80% yield) was analyzed by NMR spectroscopy and the structure confirmed. $^1$H NMR (DMSO-$d_6$): $\delta$ 1.08 (t, 3H, $CH_3$), 1.86 (s, 3H, $CH_3$), 3.38 (q, 2H, $CH_2$), 3.58 (t, 2H, $CH_2$), 4.22 (t, 2H, $CH_2$), 5.69 (s, 1H, vinyl), 6.01 (s, 1H, vinyl), 6.58 (t, 1H, ArH), 6.71 (d, 2H, ArH), 7.13 (t, 2H, ArH).

**Table 1. Data for Azobenzimidazole Polymers**

| polymer | $M_w/M_n$ | $T_g$ (DSC) | $N$ ($\times 10^{21}$/cm$^3$) | $n$ | |
|---|---|---|---|---|---|
| **1** | 36 300/21 200 | 128 | 1.3 | 1.615 | 1580 nm |
| | | | | 1.622 | 1300 nm |
| | | | | 1.663 | 790 nm |
| **2** | 40 000/20 000 | 151 | 1.6 | 1.632 | 1580 nm |
| | | | | 1.640 | 1300 nm |
| | | | | 1.682 | 790 nm |
| BI–HDT | | | 0.9 | 1.581 | 1580 nm |
| | | | | 1.587 | 1300 nm |
| | | | | 1.619 | 790 nm |

**Polymer 1.** Compound **13** (5.97 g) was dissolved in 40 mL of dry *N*-methylpyrrolidinone in a 100-mL round-bottom flask containing a magnetic stirrer. 2,2'-Azobis(2-methylpropionitrile) (AIBN) (0.30 g) was added. The flask was fitted with a reflux condenser and purged with nitrogen for 15 min and then placed in an oil bath at 80 °C. The mixture was stirred 18 h at 80 °C. The solution was cooled to room temperature, and the orange polymer was precipitated by pouring the solution into cold ethanol. The polymer was rinsed with ethanol until the washings were colorless. The yield was 4.97 g or 83%. $^1$H NMR (DMSO-$d_6$): $\delta$ 8.5 (br, 1H, ArH), 8.1 (br, 1H, ArH), 8.0 (br, 2H, ArH), 7.9 (br, 3H, ArH), 7.8 (br, 2H, ArH), 7.3 (br, 1H, NH), 6.8 (br, 2H, ArH), 5.1 (s, 1H, OH), 4.4–3.7 (br, 7H, $CH_2$), 3.6 (br, 2H, $CH_2$), 3.4 (br, 2H, $CH_2$), 3.3 (br, 2H, $CH_2$), 2.2–1.5 (br, 3H, $CH_3$), 1.40–0.7 (br, 8H, $CH_2$, $CH_3$).

**Polymer 2** was synthesized analogously from compound **12**. $^1$H NMR (DMSO-$d_6$): $\delta$ 8.5 (br, 1H, ArH), 8.1 (br, 1H, ArH), 8.0 (br, 2H, ArH), 7.9 (br, 3H, ArH), 7.8 (br, 2H, ArH), 6.8 (br, 2H, ArH), 5.1 (s, 1H, OH), 4.5–3.9 (br, 5H, $CH_2$), 3.9–3.2 (br, 4H, $CH_2$), 2.2–1.5 (br, 3H, $CH_3$), 1.4–0.5 (br, 8H, $CH_2$, $CH_3$). Molecular weight and $T_g$ data for polymers **1** and **2** are shown in Table 1. Polymer molecular weights were measured by gel permeation chromatography using polystyrene standards. Glass transition temperatures ($T_g$) were determined with a Perkin-Elmer Series 7 thermal analysis system using a heating rate of 10 °C/min.

**Film Formation and Poling.** Side-chain, guest–host, and cross-linked polymer films containing azobenzimidazole dye were prepared for optical studies. All films were spin-coated at 2000 rpm for 30 s from solutions filtered through 0.2-$\mu$m filters. Polymers **1** and **2** were coated from a pyridine solution containing 17 wt % polymer to yield films 1.3–1.5 $\mu$m thick. Guest–host polymer films 2.6 $\mu$m thick were coated from solutions prepared by dissolving 30 mg of BI and 270 mg of PMMA (Polysciences Inc., MW 75 000) in 1.5 mL of pyridine. All films were dried 2 h at 75 °C prior to poling.

Formation of cross-linked polyurethane or poly(urea–urethane) polymers was performed by dissolving a difunctional azobenzimidazole compound (BI or BIN2) in pyridine (freshly distilled from calcium hydride) along with 10% equivalent excess Tolonate HDT (the triisocyanate isocyanurate made from 1,6-hexamethylene diisocyanate, used as obtained from Rhone-Poulenc). A small amount of the surfactant FC 430 (3M Co.) was added to improve film quality. The solution was precured under conditions specified hereafter and then was filtered and spin-coated under clean conditions onto glass substrates with indium tin oxide (ITO) electrodes. The 2.5–3.5-$\mu$m films were dried at 75 °C prior to poling. Progress of cross-linking reactions was followed in films coated onto salt plates by IR spectra measured on a Perkin-Elmer Model 983 infrared spectrophotometer.

Contact poling was performed by applying a dc voltage across heated films having either sputtered ITO or vapor-deposited gold top electrodes. ITO electrodes were employed in experiments in which second-harmonic coefficients ($d_{33}$) were determined and gold electrodes were used in depoling experiments and in the determination of electrooptic coefficients ($r_{33}$).

**SHG Measurements.** Second-harmonic generation of poled films was measured using a fundamental wavelength of 1580 nm. Generation of incident laser pulses and detection of the 790-nm harmonic signal have been described elsewhere.[25] Film samples were poled in an oven through which the laser beam passed, with the film normal making a 45° angle with respect to the *p*-polarized beam. SHG from a quartz crystal ($d_{11}$ = 0.5 pm/V) served as a reference in the determination of $d_{33}$ values for poled films.

**Electrooptic ($r_{33}$) Stability Measurements.** BIN2–HDT films were prepared as described above, using a 15 min/50 °C precure and a 1 h/75 °C drying step. The BIN2–HDT samples were poled at 1 MV/cm and simultaneously cured, first at 109 °C for 35–50 min and then at 122 °C for a 2 h period. After poling, the BI–HDT films were cooled to room temperature at a rate of 2–3 °C/min, and a base-line electrooptic (EO) measurement was made. EO coefficients for the samples were obtained at 1300 nm wavelength using a transmission measurement described in the literature.[25,38] The modulation voltage was 5 $V_{rms}$ at 680 Hz. The films were stored in air in ovens maintained at constant temperature and were only removed for EO measurements to monitor changes in the second-order nonlinearity of the films. The samples were allowed to reach room temperature before measurement.

**UV–Visible Thermal Stability Measurements.** Thermal stability of the azo benzimidazole chromophore was tested by storing films of BIN2–HDT at 100 and 110 °C in air and monitoring the UV–visible absorbance from 350 to 700 nm with a Shimadzu UV 3101 spectrophotometer. Care was taken to avoid exposure of the films to ambient light during testing.

**Concentration and Refractive Index Determination.** Number densities of azobenzimidazole chromophores in polymer films were based on the known weight fraction of the chromphore in its respective polymer matrix (i.e., guest–host, side-chain, or cross-linked) and on the density of the thin film estimated from weight and volume determinations for a given sample. Refractive indices at 790, 1300, and 1580 nm were obtained by fitting transmittance spectra of polymer films coated onto quartz substrates. Spectra were measured in the near-infrared on a Shimadzu UV3101 spectrophotometer, and fitting employed the Sellmeier dispersion formula.[39] By fitting transmittance values throughout the spectrum, both the refractive index and film thickness were uniquely determined. Thicknesses obtained in this manner were in good agreement with values measured with an Alpha-Step 200 from Tencor Instruments.

**Device Fabrication.** A Mach–Zehnder (MZ) device was fabricated by photobleaching and poling in a manner similar to that reported for RA–HDT.[25] Three film layers were applied to a gold-coated silicon substrate by spin coating. The UV curable adhesive Norland 61 was used for top and bottom buffer layers. The BIN2–HDT guiding layer was photobleached by visible light from a Xenon lamp to define the 500-$\mu$m gap MZ prior to application of the top buffer layer and poling. The two arms of the MZ were poled in opposite directions, each being maintained at 2.4 MV/cm and 122 °C for 2 h. The effective field across the guiding layer was estimated by accounting for conductivity of the buffer layers obtained from separate measurements. The total device thickness was 9.9 $\mu$m, with an electrode length of 12 mm.

## Results and Discussion

The azobenzimidazole compounds were synthesized according to Scheme 1. The synthesis of the azobenzimidazoles was very versatile, and compounds with many different combinations of functionalities were obtained. Due to the variety of functional groups which could be included, the azobenzimidazole molecule could be incorporated into many different types of polymers. Substitution of a different functionality could be used to adjust the kinetics of reaction of the molecule with comonomers, such as the trifunctional isocyanate used here.

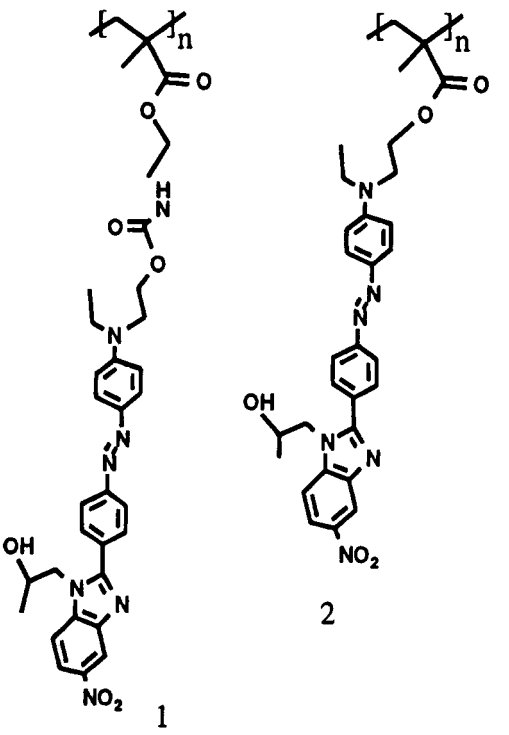


**Figure 1.** Side-chain polymers.

Polymerization of methacrylate-functional azobenzimidazoles into the homopolymers shown in Figure 1 was straightforward, yielding polymers of suitable molecular weight. Number densities of the NLO chromophore in films made from the neat polymers were relatively high, as were the resulting refractive indices, $n$. These data are shown in Table 1. It was also possible to cross-link the polymers through the pendant OH group on the side chains.

SHG coefficients were measured from polymers **1** and **2** while poling them at 110 and 144 °C, respectively, between parallel electrodes under an electric field of 1.0 MV/cm. Poling at higher temperatures produced no further increase in SHG intensity. The $d_{33}$ value obtained for polymer **1** and 13 pm/V, 20% lower than the 16.5 pm/V value measured for polymer **2**. This percent change corresponds to the difference in number density of the azobenzmidazole chromophore in these two polymers. Films of polymers **1** and **2** poled in a similar manner and cooled slowly (3–5 °C/min) to room temperature were subsequently subjected to a linear temperature ramp (3 °C/min) with the electric field removed and electrodes short-circuited. By simultaneously monitoring SHG and short-circuit current during heating, the films were found to depole at 107 and 132 °C, respectively, as determined from the temperature at which the depoling current peaked and the corresponding point of steepest decline of $d_{33}$. The variation in depoling temperature ($T_d$) for polymers **1** and **2** correlates with the difference in $T_g$ observed for these materials by DSC (Table 1). The $T_d$ values are lower than their $T_g$ counterparts in part due to the slower temperature ramp employed in the depoling experiments.

The compound BI, having one primary and one secondary hydroxyl group, could be reacted with HDT to form a cross-linked polyurethane network. Since the secondary hydroxyl groups react with isocyanate more slowly than does a primary hydroxyl group, precuring, coating, and drying the films at sufficiently low tem-

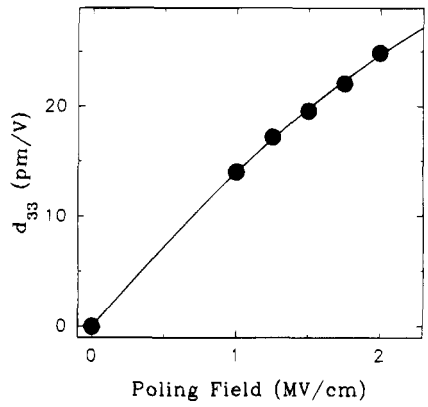


**Figure 2.** Second-harmonic coefficients determined for BI–HDT as a function of poling field. The solid line is a guide to the eye.

peratures left one end of the BI dyes free so that the chromophores could be oriented while poling and simultaneously curing the films at high temperature. By monitoring the isocyanate band (2270 $cm^{-1}$) in the IR spectrum, it was determined that precuring for 1 h at 50 °C prior to coating and drying for 2 h at 75 °C after coating consumed 40–45% of the isocyanate required to react both hydroxyl groups in BI. The appearance of an IR band at 1710 $cm^{-1}$ and increased intensity near 1520 and 1240 $cm^{-1}$ indicated that urethane linkages had been formed at this stage. After spin-coating and curing films for 1.5 h at 150 °C, a total of 90% equivalent isocyanate had reacted, increasing the concentration of urethane linkages. IR spectra revealed no further production of urethane linkages when heating more than 1.5 h. Due to the significant weight fraction of HDT in the films, the number density of BI dye in the cross-linked network and the associated refractive indices (Table 1) were lower than the respective values observed in the side-chain polymers described above.

In order to pole BI–HDT films without the occurrence of electrical breakdown, precuring and drying conditions had to be altered. Samples precured for 1 h at 85 °C and dried 4 or 5 h at 75 °C could be poled at 92 °C. At this stage of the process, about 70% equivalent isocyanate had reacted. The $d_{33}$ value measured while poling these films at 1.0 MV/cm was 14 pm/V. Raising the poling field stepwise up to 2.0 MV/cm yielded $d_{33}$ values as large as 25 pm/V, as displayed in Figure 2.

A comparison of SHG coefficients obtained from polymer films containing BI was made for the two side-chain polymers **1** and **2**, the cross-linked network BI–HDT, and a guest–host polymer comprising 10 wt % BI in PMMA. The $d_{33}$ values, as displayed in Table 2, were obtained from samples while poling at $E_{pol} = 1.0$ MV/cm at the temperatures ($T_{pol}$) indicated. Interpretation of the data was based on the relationship[40]

$$d_{33} \propto \left[\frac{NF_{SHG}E_{pol}}{T_{pol}}\mu\beta_{SHG}\right] \quad (1)$$

where $N$ is the number density of BI in the film and $F_{SHG}$ is the local field correction factor, given by

$$F_{SHG} = f^{2\omega}f^{\omega}f^{\omega}f^{0} \quad (2)$$

Here, we take $f^{\omega} = (n_{\omega}^2 + 2)/3$ and $f^0 = (n^2 + 2)/(n^2/\epsilon + 2)$ and estimate $\epsilon$, the static dielectric constant, from literature values suggested for films during poling.[41] The $\mu\beta_{SHG}$ factor, a product of the dipole moment and the molecular hyperpolarizability, was assumed to be constant from film to film. Calculated ratios of $d_{33}$ values for different films were obtained from determinations of the parameters in brackets in eq 1 and compared to the corresponding ratios of measured values, as displayed in Table 2.

**Table 2. SHG Poling Data for BI-Containing Polymers**

| film | BI/PMMA | BI–HDT | polymer **1** | polymer **2** |
|---|---|---|---|---|
| $T_{pol}$ (°C) | 92 | 92 | 110 | 144 |
| $d_{33}$ (pm/V) | 2.8 | 13.5 | 13.0 | 16.5 |
| $d_{33}/d_{33}$(BI/PMMA) (exptl) | 1.0 | 4.8 | 4.7 | 5.9 |
| $d_{33}/d_{33}$(BI/PMMA) (calcd) | 1.0 | 8.5 | 11.7 | 14.8 |

As is observed from the tabulated ratios, the $d_{33}$ values measured for the cross-linked and side-chain polymer films are significantly lower than those predicted by extrapolation of the $d_{33}$ value obtained for the guest–host BI/PMMA film. The $d_{33}$ measured from BI–HDT is more than 40% lower than the expected result, and measured values for polymers **1** and **2** are 60% lower than anticipated. Limiting factors that cause lower than expected $d_{33}$ values may include restricted dye mobility due to attachment at (at least) one end of the molecule or centrosymmetric aggregation of the dye in highly concentrated films. It is interesting to note that the ratio of $d_{33}$ values measured for the two side-chain polymers is in excellent agreement with the calculated ratio, suggesting that whatever is preventing the measured $d_{33}$ from approaching the predicted values is common to these two polymer films. Data obtained in a similar study in which RA was the NLO dye incorporated into the films produced essentially the same results: The measured $d_{33}$ for RA–HDT was about 40% lower than the extrapolated value, and the measured $d_{33}$ for an RA analog of polymer **1** was more than 70% lower than the expected result. Thus, the polymer backbone and the mode and extent of chromophore attachment (if any) appear to play a significant role in limiting the nonlinearity achievable in side-chain and cross-linked NLO films.

Complete cross-linking of BI–HDT while poling required that the film temperature be raised above 100 °C; however, this led to electrical breakdown which damaged the films. In contrast, it was determined that the BIN2 compound, which has different functional groups while retaining the azobenzimidazole chromophore, could be substituted for BI to produce excellent films that did not suffer breakdown during poling and curing. Chromophore number density and film refractive indices in BIN2–HDT were essentially identical to those observed in BI–HDT.

The stepwise reaction of BIN2 with Tolonate HDT was studied by IR spectroscopy in the same manner as BI. The reaction was similar to the reaction of RA with HDT; the amine reacts much faster with the isocyanate than the hydroxyl, so the reaction can be performed in two steps. IR spectra were obtained at three points in the cross-linking process: (1) immediately after spin-coating a solution precured for 15 min/50 °C, (2) after the 1 h/75 °C drying step, and (3) after full cure (35–50 min at 109 °C, 2 h at 122 °C). After the spin-coating step, quantitative monitoring of the isocyanate band (2270 $cm^{-1}$) revealed that just under 50% equivalent of the Tolonate HDT had been consumed. This result indicates that the amine reaction nearly reaches completion during processing prior to spin coating. A peak observed at 1550 $cm^{-1}$ indicated the formation of urea. The IR spectra of BIN2–HDT films after the 1 h/75 °C

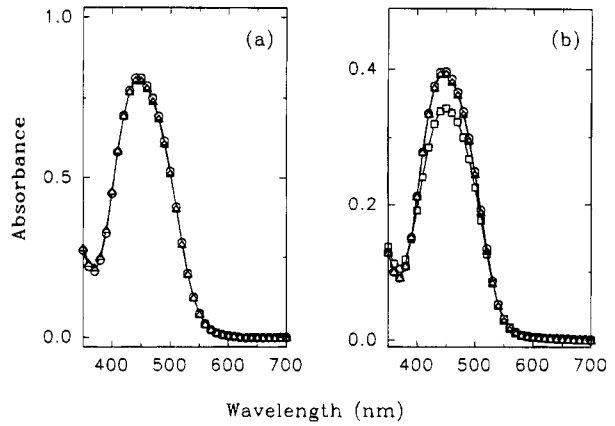


**Figure 3.** (a) UV–visible spectrum of a BIN2–HDT film before (circles) and after (triangles) storage for 27 days at 100 °C. (b) UV–visible spectrum of a BIN2–HDT film before light exposure (circles), after 45 min of exposure to room light at room temperature (squares), and after storage in the dark for 4 days at 100 °C (triangles).

drying step show a further decrease in NCO and peaks at approximately 1720, 1530, and 1260 $cm^{-1}$ due to formation of some urethane. Generation of urethane linkages by reaction of the OH and NCO groups is also reflected in changes in the CO bands at about 1060 $cm^{-1}$. The curing step reacts an amount of isocyanate nearly sufficient to cross-link all OH groups.

The thermal stability of BIN2–HDT films that were cured but not poled was examined by monitoring UV–visible spectra of the films. The results are shown in Figure 3. When the films were stored in the dark at 100 °C in air, only a 1% decrease in the peak UV–visible absorbance at 445 nm was observed after 27 days, as is shown by a comparison of the curves in Figure 3a. Similar tests on a sample held at 110 °C revealed comparable stability in the peak absorbance over a few days. In contrast, when the films were left at room temperature under ambient room light for less than an hour, a reversible decrease in UV–visible absorbance was observed as shown in Figure 3b. Storing the film in the dark at 100 °C allowed complete recovery of the original spectrum. The light-induced decrease in intensity of the absorbance band at 445 nm and concomitant increase in absorbance at shorter wavelengths, together with the thermal reversibility of these spectral features, are consistent with a *trans–cis* isomerization which has been reported in other azo dyes.[42]

Electrooptic (EO) measurements on films of BIN2–HDT that were poled and cured under 1 MV/cm fields yielded electrooptic coefficients ($r_{33}$) in the range of 6–8 pm/V at 1300 nm. Larger values of $r_{33}$ approaching 15 pm/V were obtained from films poled under fields exceeding 2.5 MV/cm.

Stability of the EO response was monitored for BIN2–HDT films maintained in ovens under ambient atmosphere at 85, 100, and 110 °C. Figure 4 displays the normalized $r_{33}$ values of these films measured over a period of up to 2 months. It is interesting to note that at temperatures up to 100 °C, the films retain greater than 80% of the initial $r_{33}$ value for a period of more than 60 days, but at a temperature just 10 °C higher, the EO response greatly diminishes in less than 1 day. Together these results not only imply that the $T_g$ of the films is just above 110 °C but also suggest that the energy barrier for relaxation of the poled dyes is sufficiently high to minimize decay of EO response in devices made from these materials.

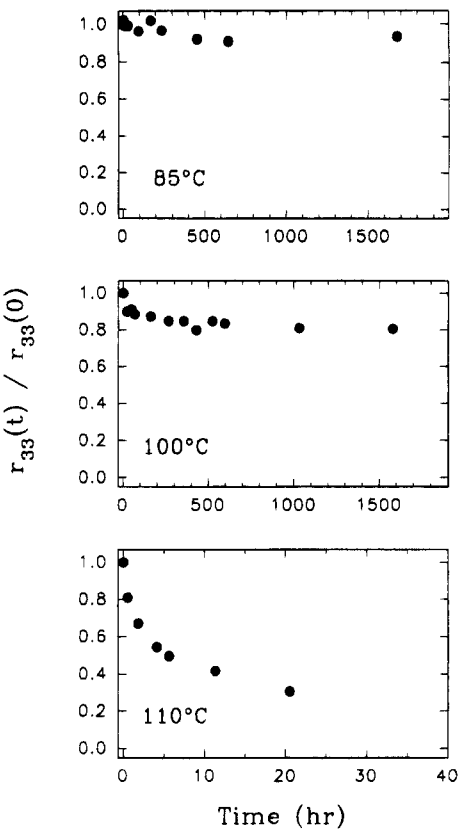


**Figure 4.** Stability of the electrooptic coefficient of BIN2–HDT films stored at 85, 100, and 110 °C.

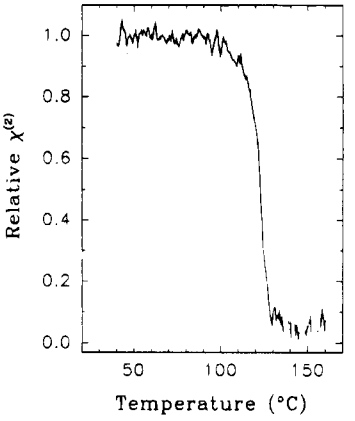


**Figure 5.** Relative $\chi^{(2)}$ response of a BIN2–HDT film heated at 2.5 °C/min. Since the data were obtained as $I_{SHG}^{1/2}$, noise in the SHG measurement at low signal levels produced breaks in the curve where $I_{SHG} < 0$.

The depoling behavior of the BIN2–HDT films is illustrated in Figure 5, where SHG intensity ($I_{SHG}$) was monitored during the application of a linear temperature ramp. When the sample is heated at 2.5 °C/min, the relative $\chi^{(2)}$ value (obtained as $(I_{SHG})^{1/2}$) sharply decreases to zero above 110 °C, with the point of sharpest decrease occurring at 122 °C. This depoling temperature corroborates the suggestion above that $T_g$ of the BIN2–HDT material is just above 110 °C. The decrease of $\chi^{(2)}$ completely to zero is in contrast to the result for cross-linked polymers reported elsewhere[24,29] which retained some $\chi^{(2)}$ activity above the depoling temperature.

Photobleaching of BIN2–HDT was examined as a convenient method for fabrication of optical waveguides.[43] Bleaching of BIN2–HDT at high incident intensities (8 $mW/cm^2$ or more at 365 nm) was found to be irrevers-

ible. The index of refraction of a fully bleached BIN2–HDT film was 1.560 at 1300 nm.

Linear propagation loss in BIN2–HDT was measured at 1300 nm in both photobleached and V-groove single-mode optical waveguides. The loss was typically 3.0 dB/cm. The loss decreased to about 2.0 dB/cm if the 1 h/75 °C drying step was eliminated and the sample was instead baked at 120 °C for 2 h immediately after spin coating. A subsequent annealing of the sample at room temperature for 10 days reduced the loss to 1.2 dB/cm. The best Mach–Zehnder (MZ) device that incorporated BIN2–HDT exhibited an $r_{33}$ of 13.1 pm/V at 1300 nm, and the measured $V_\pi$ was 10 V with a modulation depth of better than 90%.

**Acknowledgment.** We thank A. Isackson for sample preparation, P. Kitipichai for synthetic efforts, R. Newmark and D. Weil for analytical measurements, and G. Boyd for helpful discussions.

**Supplementary Material Available:** Additional NMR and mp data for azobenzimidazole compounds and intermediates (4 pages). Ordering information is given on any current masthead page.

## References and Notes

(1) Park, J.; Marks, T. J.; Yang, J.; Wong, G. K. *Chem. Mater.* **1990**, *2*, 229.
(2) Jin, Y.; Carr, S. H.; Marks, T. J.; Lin, W.; Wong, G. K. *Chem. Mater.* **1992**, *4*, 963.
(3) Chen, M.; Dalton, L. R.; Yu, L. P.; Shi, Y. Q.; Steier, W. H. *Macromolecules* **1992**, *25*, 4032.
(4) Chen, M.; Yu, L. P.; Dalton, L. R.; Shi, Y. Q.; Steier, W. H. *Macromolecules* **1992**, *24*, 5421.
(5) Muller, H.; Muller, I.; Nuyken, O.; Strohriegl, P. *Makromol. Chem., Rapid. Commun.* **1992**, *13*, 289.
(6) Yu, L.; Chan, W.; Dikshit, S.; Bao, Z.; Shi, Y.; Steier, W. H. *Appl. Phys. Lett.* **1992**, *60*, 1655.
(7) Jeng, R. J.; Chen, Y. M.; Chen, J. I.; Kumar, J.; Tripathy, S. K. *Macromolecules* **1993**, *26*, 2530.
(8) Marturunkakul, S.; Chen, J. I.; Li, L.; Jeng, R. J.; Kumar, J.; Tripathy, S. K. *Chem. Mater.* **1993**, *5*, 592.
(9) Shi, Y.; Steier, W. H.; Chen, M.; Yu, L.; Dalton, L. R. *Appl. Phys. Lett.* **1992**, *60*, 2577.
(10) Kawatsuki, N.; Schmidt, H.-W.; Pakbaz, K. *J. Appl. Polym. Sci.* **1993**, *50*, 1575.
(11) Cheng, L.-T.; Foss, R. P.; Meredith, G. R.; Tam, W.; Zumsteg, F. C. *Mol. Cryst. Liq. Cryst. Sci. Technol., Sect. B* **1993**, *4*, 211.
(12) Chen, Y. M.; Jeng, R. J.; Li, L.; Zhu, X.; Kumar, J.; Tripathy, S. *Mol. Cryst. Liq. Cryst. Sci. Technol., Sect. B* **1993**, *4*, 71.
(13) Hayashi, A.; Goto, Y.; Nakayama, M.; Sato, H.; Watanabe, T.; Miyata, S. *Macromolecules* **1992**, *25*, 5094.
(14) Eich, M.; Reck, B.; Yoon, D. Y.; Willson, C. G.; Bjorklund, G. C. *J. Appl. Phys.* **1989**, *66*, 3241.
(15) Jungbauer, D.; Reck, B.; Tweig, R.; Yoon, D. Y.; Willson, C. G.; Swalen, J. D. *Appl. Phys. Lett.* **1990**, *56*, 2610.
(16) Hubbard, M. A.; Marks, T. J.; Lin, W.; Wong, G. K. *Chem. Mater.* **1992**, *4*, 965.
(17) Mandal, B. K.; Kumar, J.; Huang, J.-C.; Tripathy, S. K. *Makromol. Chem., Rapid Commun.* **1991**, *12*, 63.
(18) Xu, C.; Wu, B.; Dalton, L. R.; Shi, Y.; Ranon, P. M.; Steier, W. H. *Macromolecules* **1992**, *25*, 6714.
(19) Xu, C.; Wu, B.; Dalton, L. R.; Ranon, P. M.; Shi, Y.; Steier, W. H. *Macromolecules* **1992**, *25*, 6716.
(20) Xu, C.; Wu, B.; Becker, M. W.; Dalton, L. R.; Ranon, P. M.; Shi, Y.; Steier, W. H. *Chem. Mater.* **1993**, *5*, 1439.
(21) Xu, C.; Wu, B.; Todorova, O.; Dalton, L. R.; Shi, Y.; Ranon, P. M.; Steier, W. H. *Macromolecules* **1993**, *26*, 5303.
(22) Shi, Y.; Ranon, P. M.; Steier, W. H.; Xu, C.; Wu, B.; Dalton, L. R. *Appl. Phys. Lett.* **1993**, *63*, 2168.
(23) Wu, B.; Xu, C.; Ra, Y.; Dalton, L. R.; Kalluri, S.; Shi, Y.; Steier, W. H. *Polym. Prepr. (Am. Chem. Soc., Div. Polym. Chem.)* **1994**, *35* (1), 494.
(24) Beecher, J. E.; Frechet, J. M. J.; Willand, C. S.; Robello, D. R.; Williams, D. J. *J. Am. Chem. Soc.* **1993**, *115*, 12216.
(25) Francis, C. V.; White, K. M.; Boyd, G. T.; Moshrefzadeh, R. S.; Mohapatra, S. K.; Radcliffe, M. D.; Trend, J. E.; Williams, R. C. *Chem. Mater.* **1993**, *5*, 506.
(26) Francis, C. V.; Cross, E. M.; Harelstad, R. E.; Korkowski, P. F.; Leung, P. C.; Macomber, D. W.; Trend, J. E. U.S. Patent 5 256 784.
(27) White, K. M.; Francis, C. V.; Isackson, A. J. *Macromolecules* **1994**, *27*, 3619.
(28) Harelstad, R. E.; Francis, C. V.; Leung, P. C.; Korkowski, P. F.; White, K. M.; Cross, E. M.; Kitipichai, P. In *Electrical, Optical, and Magnetic Properties of Organic Solid State Materials*; Garito, A. F., Jen, A. K.-Y., Lee, C. Y.-C., Dalton, L. R., Eds.; Symposium Proceedings; Materials Research Society: Pittsburgh, 1994; Vol. 328, p 637.
(29) Twieg, R. J.; Betterton, K. M.; Burland, D. M.; Lee, V. Y.; Miller, R. D.; Moylan, C. R.; Volksen, W.; Walsh, C. A. *Proc. SPIE* **1993**, *2025*, 94.
(30) Beeson, K. W.; Ferm, P. M.; Horn, K. A.; Knapp, C. W.; McFarland, M. J.; Nahata, A.; Shan, J.; Wu, C.; Yardley, J. T. *Proc. SPIE* **1993**, *2025*, 488.
(31) Ermer, S.; Valley, J. F.; Lytel, R.; Lipscomb, G. F.; van Eck, T. E.; Girton, D. G. *Appl. Phys. Lett.* **1992**, *61*, 2272.
(32) White, K. M.; Cross, E. M.; Francis, C. V. *Polym. Prepr. (Am. Chem. Soc., Div. Polym. Chem.)* **1994**, *35* (2), 172.
(33) Cassidy, P. E. *Thermally Stable Polymers*; Marcel Dekker: New York, 1980.
(34) Preston, N. P. *Chem. Rev.* **1974**, *74*, 279.
(35) Patai, S., Ed. *The Chemistry of Diazonium and Diazo Groups*; John WIley and Sons: New York, 1978.
(36) Stevens, F. F.; Bower, J. D. *J. Chem. Soc.* **1950**, 1722.
(37) Fazio, M. *J. Org. Chem.* **1984**, *49*, 4889.
(38) van der Vorst, C. P. J. M.; van Weerdenburg, C. J. M. *Proc. SPIE* **1990**, *1337*, 246.
(39) Wood, R. W. *Physical Optics*, 3rd ed.; Optical Society of America: Washington, DC, 1988.
(40) Singer, K. D.; Sohn, J. E.; Lalama, S. *J. Appl. Phys. Lett.* **1986**, *49*, 248.
(41) Page, R. H.; Jurich, M. C.; Reck, B.; Sen, A.; Twieg, R. J.; Swalen, J. D.; Bjorklund, G. C.; Wilson, C. G. *J. Opt. Soc. Am. B* **1990**, *7*, 1239.
(42) Loucif-Saïbi, R.; Nakatani, K.; Delaire, J. A.; Dumont, M.; Sekkat, Z. *Chem. Mater.* **1993**, *5*, 229.
(43) Rochford, K. B.; Zanoni, R.; Gong, Q.; Stegeman, G. I. *Appl. Phys. Lett.* **1989**, *55*, 1161.

MA941205T